

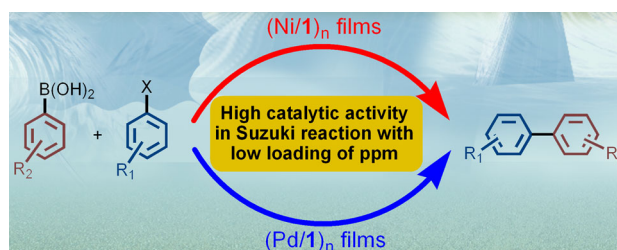
Pd- and Ni-Pyridyl Complexes Deposited as Films for Suzuki–Miyaura and Mizoroki–Heck Cross Coupling Reactions

Xiuhua Zhao¹ · Jie Zhang² · Yayun Zhao² · Xing Li²

Received: 28 June 2015 / Accepted: 26 August 2015
© Springer Science+Business Media New York 2015

Abstract A pyridyl fluorene ligand, 2,7-bis(4-pyridyl)-9,9-diethylfluorene (**1**), has been synthesized by a simple route. The ability of the two linearly terminal pyridyl nitrogen atoms of **1** to coordinate with the Pd(II) or Ni(II) ions has enabled the use of **1** as a linking ligand in the preparation of $(\text{PdCl}_2/\mathbf{1})_n$, $(\text{Ni}(\text{NO}_3)_2/\mathbf{1})_n$ films, $\text{PdCl}_2/\mathbf{1}$ and $\text{Ni}(\text{NO}_3)_2/\mathbf{1}$ complex. The resulting films and complexes were characterized by UV–vis spectroscopy, atomic force microscopy, X-ray photoelectron spectroscopy, scanning electron microscopy, transmission electron microscopy and energy dispersive X-ray spectrometer. The application of films and complexes as catalysts for Suzuki–Miyaura and Mizoroki–Heck reactions was carried out. $(\text{PdCl}_2/\mathbf{1})_n$ films show high catalytic activity in the reactions with the Pd loading of ppm. $(\text{Ni}(\text{NO}_3)_2/\mathbf{1})_n$ multilayers as the active catalytic moieties for these reactions were investigated with very low Ni(II)-loading.

Graphical Abstract The $(\text{Pd or Ni}/\mathbf{1})_n$ multilayer films were used as high active catalysts for the C–C formation with extremely low M(II)-loading in ppm level.



Keywords Palladium · Nickel · Multilayer films · Catalysis · Suzuki–Miyaura and Mizoroki–Heck reactions

Electronic supplementary material The online version of this article (doi:10.1007/s10562-015-1614-4) contains supplementary material, which is available to authorized users.

✉ Xing Li
lixing@nbu.edu.cn; lix905@126.com

Xiuhua Zhao
1017027635@qq.com

Jie Zhang
1347582628@qq.com

Yayun Zhao
1390617347@qq.com

¹ Faculty of Science, Ningbo University, Ningbo 315211, Zhejiang, People's Republic of China

² Faculty of Materials Science and Chemical Engineering, Ningbo University, Ningbo 315211, Zhejiang, People's Republic of China

1 Introduction

The transition-metal-catalyzed cross-coupling reactions such as Suzuki–Miyaura [1], Mizoroki–Heck [2], Stille [3–5], Kumada [6], Negishi [7, 8], Hiyama [9] and Sonogashira [10] reactions are very powerful tools for the C–C bonds formation. These methods have been extensively used in a wide range of academic areas including biological materials and medicinal product synthesis. Among the powerful transformations, the traditional palladium-catalyzed Suzuki–Miyaura and Mizoroki–Heck reactions represent the important ones with phosphine ligand in the presence of a suitable base under an inert atmosphere [11–15]. However, phosphine ligands are toxic and air-sensitive [16, 17]. Therefore, large-scale industrial application is limited for Pd-P catalysts, and the development of phosphine-free catalysts for C–C bond formation reactions has

become a current focus [18, 19]. Yu [20] and Özdemir [21] reported that bidentate 1,10-phenanthroline and dialkylimidazolium were used as the ligand to activate the Pd(II)-catalysts, respectively. The phosphine-free Pd-catalyst is a luxurious case in the industrial organic synthesis since Pd and its complexes are very expensive materials, even which show high catalytic activity with a high Pd-loading of 3–10 mol%. Subsequently, Pd–Pt multilayer films were successfully assembled with the extra-low Pd loading, which as catalysts in the Suzuki–Miyaura coupling reaction showed considerable high catalytic activity [22, 23]. However, the application of Pd–Pt-organometallic catalysts was greatly restricted in the organic synthesis because of its high cost and strict preparation process. Wang [24] and Monteiro [25] demonstrated that the Ni(TFA)₂ with β-diketone and PPh₃ ligands, or the ligand-free NiCl₂·6H₂O could be used to catalyze the coupling reactions of a certain scope of aryl bromides and iodides with aryl boronic acids, but it's a pity that the Ni(II)-loading is up to 10 mol% in those reaction above. In this report, we synthesized a new pyridyl fluorene ligand, namely, 2,7-bis(4-pyridyl)-9,9-diethylfluorene (**1**, Scheme 1), which was used to assemble the multilayer films by alternating adsorption metal ions (Pd or Ni) and **1** onto the quartz slide [26–32]. The (PdCl₂/**1**)_n, (Ni(NO₃)₂/**1**)_n films catalysts showed high catalytic activity in the Suzuki–Miyaura and Mizoroki–Heck reactions with the metal loading in ppm level.

2 Experimental Section

2.1 Materials and Methods

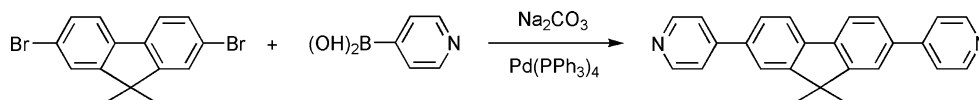
All catalysis coupling reactions were carried out under air atmosphere. All other synthetic reactions were performed by using standard Schlenk techniques utilizing a double-manifold vacuum system with high purity nitrogen flow. Poly(ethylenimine) (abbreviated as PEI) was purchased from Aldrich Chemical Company. All solutions were prepared with doubly-distilled water. All reagents were of analytical grade and used as received without further purification. Infra-red spectra were recorded on a Nicolet Avatar FTIR spectrophotometer in the range 4,000–400 cm⁻¹ (1 cm⁻¹ resolution, 16 scans). NMR spectra were obtained from solutions in CDCl₃ using Bruker DRX-400 spectrometers. Gas chromatography-mass spectrometry

(GC–MS) was performed on a 430 GC (Varian, USA). UV–vis absorption spectra were recorded on a quartz slide using a Lambda35 spectrophotometer (Perkin Elmer, USA). High-resolution X-ray photoelectron spectra (XPS) were collected at a takeoff angle of 45° using PHI Quantum 2000 scanning ESCA microprobe (Physical Electronics, USA) with an AlKα X-ray line (1486.6 eV). Atomic force microscope (AFM) images were taken on a single-crystal silicon slide using a Veeco Multimode NS3A-02NanoscopeIII atomic force microscope with silicon tips. Height images of the films were recorded using tapping-mode AFM. Analysis of Pd content was measured by inductively coupled plasma-atomic emission spectroscopy (ICP-AES) using Ultima. Transmission electron microscopy (TEM) images were carried out by Tecnai G2 F20 S-TWIN. Scanning electron microscopy (SEM) images were taken with SU-70 field-emission scanning electron microscope. Energy dispersive X-ray spectrometer (EDS) was carried out on a Carl Zeiss model Ultra 55 microscope. The solid state fluorescence spectra were measured on F-4600 fluorescence spectrophotometer. Powder X-ray diffraction (PXRD) data were collected on a Bruker D8 Focus X-ray diffractometer using Cu Kα radiation.

2.2 Synthesis of 2,7-Bis(4-pyridyl)-9,9-diethylfluorene (**1**)

The samples of 2,7-dibromo-9,9'-diethylfluorene (3.0 mmol), 4-pyridine boronic acid (7.5 mmol), Na₂CO₃ (12.0 mmol) and Pd(PPh₃)₄ (0.1 mmol) were added to the 250 mL three-necked flask and dissolved in a mixture of 1,2-dimethoxy ethane (abbreviated as DME) and distilled water (80/40 mL). The resulting mixture was refluxed under N₂ atmosphere at 95 °C for 48 h, cooled to the room temperature, and extracted with dichloromethane for three times. Then the organic phase was dried over anhydrous magnesium sulfate, concentrated and purified by column chromatography on silica gel eluting with petroleum ether/ethyl acetate (1: 2) to give compound **1** as a faint yellow solid (yield: 71 %). IR (KBr, ν/cm⁻¹): 3478 (m), 3398 (w), 3028 (w), 2959 (w), 2931 (w), 2870 (vw), 2853 (vw), 1592 (vs), 1463 (s), 1408 (s), 1190 (w), 1121 (w), 1005 (w), 807 (s), 721 (w), 713 (m), 617 (w), 543 (m) cm⁻¹. ¹H NMR (CDCl₃, 400 MHz) δ: 8.69 (d, *J* = 4.8 Hz, 4H, PhH), 7.84 (d, *J* = 8.0 Hz, 2H, PhH), 7.59 ~ 7.70 (m, 8H, PhH), 2.11 (q, *J* = 56.4 Hz, 4H, CH₂), 0.40 (t, *J* = 14.4 Hz, 6H, CH₃) ppm. ESI(+)-MS (*m/z*) for [M + H]⁺: Calc. = 377.5, Obs. = 377.3.

Scheme 1 Synthesis schematic diagram of complex **1**



2.3 Layer-by-Layer Assembly of Multilayer Films

The quartz slides were cleaned with “a piranha solution” (98 % H_2SO_4 /30 % $\text{H}_2\text{O}_2 = 8:3$, V/V) at 80 °C for 40 min, and thoroughly washed with distilled water. Further purification was carried out by immersion in a $\text{H}_2\text{O}/\text{H}_2\text{O}_2/\text{NH}_4\text{OH}$ (5:2:1, V/V/V) bath at 70 °C for 30 min. Then the clean slides were first immersed in PEI solution for 20 min. Then the pre-coated PEI slides were alternatively immersed in the aqueous solution of PdCl_2 (5 mM) and ethanol solution of complex **1** (5 mM) for 30 min. The substrates were washed with water and dried after each immersion at room temperature. By repeating the above-mentioned steps, the $(\text{PdCl}_2/\mathbf{1})_n$ multilayer films were prepared. The $(\text{Ni}(\text{NO}_3)_2/\mathbf{1})_n$ films were assembled using the same method with the concentration of $\text{Ni}(\text{NO}_3)_2$ and complex **1** corresponding to 30 mM.

2.4 Preparation of Metal–Organic Complexes

The aqueous solution of PdCl_2 was quickly added to the EtOH solution compound **1** (Pd: **1** = 1: 1, mol), and the resulting mixture was stirred at 50 °C for 10 h. Then the $\text{PdCl}_2/\mathbf{1}$ complex was obtained and collected by centrifugal separation, washed alternatively with H_2O and EtOH, and dried in the air. The $(\text{Ni}(\text{NO}_3)_2/\mathbf{1})$ complex was prepared by the similar method with the temperature of 90 °C.

2.5 General Procedure for the Suzuki–Miyaura and Mizoroki–Heck Cross-Coupling Reactions

A general procedure for the coupling reaction of an aryl halide with arylboronic acid is as follows: aryl halide (1.0 mmol), arylboronic acid (1.2 mmol), K_2CO_3 (3.0 mmol), ten layers films loaded on quartz slides as catalysts, 4.0 mL H_2O and 3.0 mL EtOH were added to an flask. The reaction mixture was heated to a certain temperature in air. After the end of the reaction, the reaction system was cooled to room temperature, and extracted with ethyl acetate for three times. Then the combined organic phase was dried over anhydrous Na_2SO_4 . After removal of the solvent, the crude product was purified by silica gel column chromatography using petroleum ether to obtain the product with high purity.

For Mizoroki–Heck cross-coupling reaction, aryl halide (1.0 mmol), styrene (or t-butyl acrylate) (1.5 mmol), Na_2CO_3 (2.0 mmol), 6.0 mL *N,N*-dimethylformamide (DMF) and ten layers films loaded on quartz slides as catalysts were added to the flask. Then the resulting mixture was stirred at 140 °C for 24 h under ambient atmosphere, cooled to room temperature, and extracted with ethyl acetate for three times. The combined organic phase was

dried over anhydrous Na_2SO_4 , concentrated and purified by silica gel column chromatography with the eluent of petroleum ether.

2.6 Recycling Experiments

In the first catalytic cycle, the quartz slide coated with multilayer films was immersed into a solution of aryl halides (1.0 mmol), arylboronic acid (1.2 mmol), K_2CO_3 (3.0 mmol) in EtOH (3.0 mL) and H_2O (4.0 mL). After the mixture was stirred for 20 min at 50 °C, the quartz slide was removed and the resulting solution was heated at reflux for a further 20 h at 50 °C. Afterward, the mixture was extracted with ethyl acetate (3×15 mL). The water phase was collected and recharged with aryl halides (1.0 mmol), arylboronic acid (1.2 mmol), K_2CO_3 (3.0 mmol). EtOH (3.0 mL) and sufficient H_2O were added to make the solution volume to 7.0 mL. The coated quartz slide was re-immersed into the new reaction mixture. After the mixture was stirred for 20 min, the quartz slide was again removed from the mixture and the released metal–ligand complex was used to catalyze the second Suzuki–Miyaura reaction. By repeating these steps, the catalytic behavior of the film was investigated over several cycles.

3 Results and Discussion

3.1 UV–Vis Spectroscopy of the Multilayer Films

Through the layer-by-layer (LbL) self-assembly technique, the multilayer film is prepared by alternating adsorption of metal ion and complex **1** layers onto solid substrate pre-coated with PEI, resulting in the metal-**1** complexes loaded within multilayer films. The method is based on the coordination bond between metal ions and pyridyl N atoms from compound **1**. UV–vis spectroscopy is used to monitor the growth process of the multilayer films. The UV–vis spectra of $(\text{PdCl}_2/\mathbf{1})_n$ and $(\text{Ni}(\text{NO}_3)_2/\mathbf{1})_n$ films are shown in Figs. 1 and 2, respectively. The absorption peaks at 220 and 358 nm (Fig. 1) were observed, which could be attributed to the π – π^* transitions and n – π^* transitions of the aromatic ring, respectively. The high-energy peak at 358 nm were red-shifted compared with the one of complex **1** (Fig. S6, 330 nm), which was probably due to the charge transfer between metal and ligand or solvent effect [33]. The $(\text{PdCl}_2/\mathbf{1})_n$ film growth shows a relatively fine linear correction with $R^2 = 0.9900$ between the optical absorption at $\lambda_{\text{max}} = 358$ nm and the number of ligand layers, suggesting that the ligand is incorporated into the films with a regular growth. However, the $(\text{Ni}(\text{NO}_3)_2/\mathbf{1})_n$ film growth shows a relatively bad linear correction with $R^2 = 0.9790$ between the optical absorption at

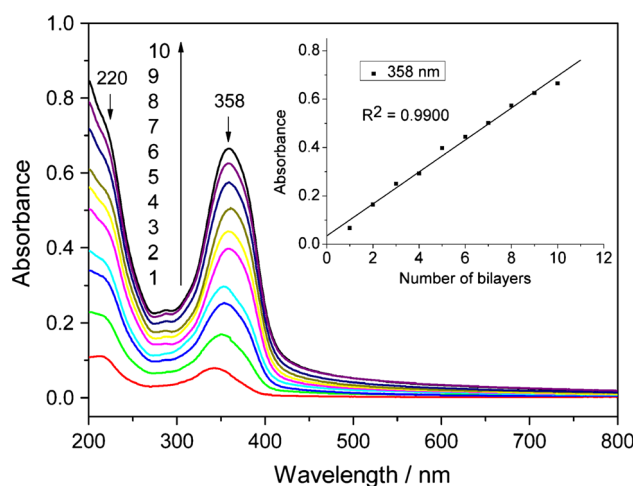


Fig. 1 UV-vis spectra of the PEI-(PdCl₂/1)_n (*n* = 1–10) films. *Inset*: increase in the absorbance at 358 nm as a function of the number of bilayers of PEI-(PdCl₂/1)_n

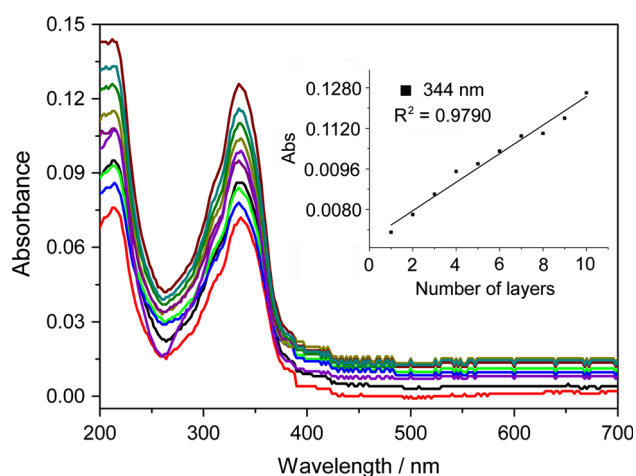


Fig. 2 UV-vis spectra of the PEI-(Ni(NO₃)₂/1)_n (*n* = 1–10) films. *Inset*: increase in the absorbance at 344 nm as a function of the number of bilayers of PEI-(Ni(NO₃)₂/1)_n

$\lambda_{\text{max}} = 344$ nm and the number of ligand layers, which indicates that the complex 1 merged into the films with a relatively irregular growth.

3.2 Analysis of Metal Content in the Multilayer Films

It is necessary for cross-couplings reactions to ascertain the metal content in multilayer films as catalysts. The on-line detection of the metal concentration can not be performed during the catalytic reaction process in our lab. A substituted method was selected to determine the amount of metal: The quartz slide coated with (PdCl₂/1)₁₀ was immersed into a NaOH aqueous solution (25 mL, 1.0 M) and UV-vis spectra were used to monitor the absorbance

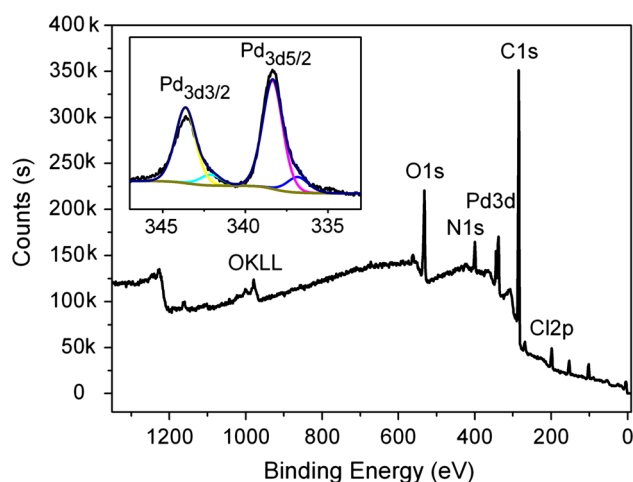


Fig. 3 XPS spectra of PEI-(PdCl₂/1)₁₀ film deposited on a single-crystal silicon substrate. *Inset*: Pd_{3d}

change of the coated quartz slide. When the coated quartz slide exhibited no absorbance, the aqueous solution (25 mL) was used for analysis of Pd content by the ICP-AES. The amount of Pd in the (PdCl₂/1)₁₀ films is determined as 9.7×10^{-4} wt % (6.3×10^{-8} mol Pd). Under similar conditions, aqueous solution of HNO₃ was used to determine the Ni content in (Ni(NO₃)₂/1)₁₀ films, and the amount of Ni in the film is 7.3×10^{-4} wt % (8.5×10^{-8} mol Ni).

XPS measurements were carried out to identify the element composition of the multilayer films deposited on the single crystal silicon substrates. As expected, the survey spectra (Fig. 3) of the (PdCl₂/1)₁₀ films showed the existence of C_{1s} (285.0 eV), Cl_{2p} (199.0 eV), N_{1s} (401.7 eV), O_{1s} (532.9 eV), OKLL (979.4 eV) and Pd_{3d} (337.8 eV), which were consistent with characteristic peaks of the corresponding elements. The shoulders of the Pd_{3d} peak on the low binding energy region were ascribed to satellite peak. Photoelectrons with energies of 338.3 eV and 343.6 eV were observed in the Inset of Fig. 3, indicating the Pd(II) oxidation state in the (PdCl₂/1)₁₀ films. Figure S8 also confirms the existence of Pd(II) in PdCl₂/1 complex.

The XPS spectra of (Ni(NO₃)₂/1)₁₀ film was also investigated. As shown in Fig. 4, the survey spectra displayed the presence of C_{1s} (285.0 eV), N_{1s} (399.2 eV), O_{1s} (532.9 eV), OKLL (981.0 eV), Ni_{2p} (856.7 eV), Si_{2s} (152.1 eV) and Si_{2p} (99.3 eV), indicating that all the expected elements were loaded in the film. The peaks of 855.3 eV and 872.9 eV on the high binding energy region were attributed to Ni_{2p3/2} and Ni_{2p1/2}, respectively, indicating the presence of Ni(II) oxidation state in the (Ni(NO₃)₂/1)₁₀ film. Figure S9 also shows that the Ni oxidation state in the Ni(NO₃)₂/1 complex is +2.

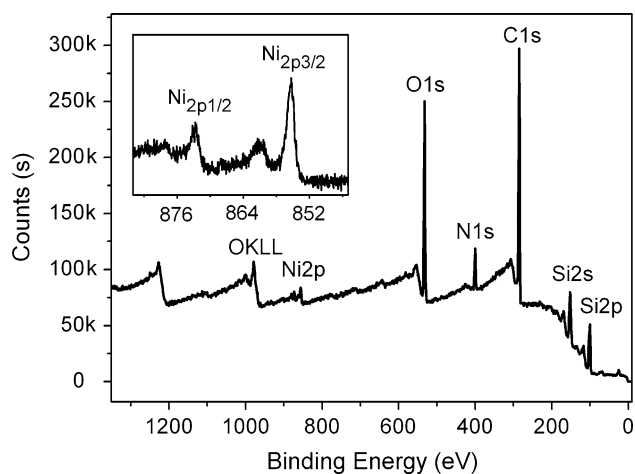


Fig. 4 XPS spectra of PEI-(Ni(NO₃)₂/1)₁₀ film deposited on a single-crystal silicon substrate. Inset: Ni_{2p}

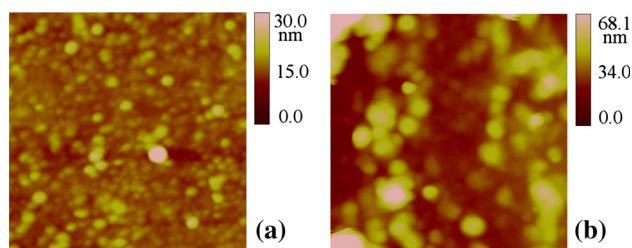


Fig. 5 AFM images of the films on the single-crystal silicon substrate (scan area is $1.0 \times 1.0 \mu\text{m}^2$); **a** and **b** are the height images of PEI-(PdCl₂/1)₅ ($R_{\text{rms}} = 2.16 \text{ nm}$) and PEI-(PdCl₂/1)₁₀ ($R_{\text{rms}} = 11.20 \text{ nm}$), respectively

3.3 Atomic Force Microscopy Images of the Multilayer Films

AFM is a powerful technique for the measurement of three-dimensional surface topography at the nanoscale. Here the AFM images of the films were used to provide detailed information of the surface morphology and homogeneity. As shown in Fig. 5a, the five-layer film of (PdCl₂/1)₅ was relatively uniform with the root-mean-square (RMS) roughness of 2.16 nm. As the number of deposited bilayers increases, large particle aggregates were observed and the island-shaped nanostructures were distributed on the surface of the (PdCl₂/1)₁₀ film with the RMS roughness of 11.20 nm, in which the average diameter of the nanoparticulate was about 60 nm (Fig. 5b). Similarly, the RMS roughness of (Ni(NO₃)₂/1)₅ and (Ni(NO₃)₂/1)₁₀ films was 2.11 and 6.17 nm (Fig. 6), respectively. And the mean diameters of nanoparticulate of five-layer and ten-layer films were 58.822 and 68.844 nm, respectively. Obviously, the RMS roughness and diameter of the films increase with the film growth in the substrate.

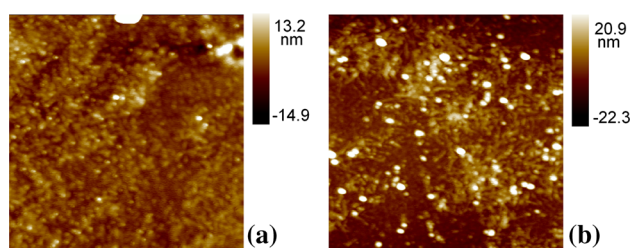


Fig. 6 AFM images of the films on the single-crystal silicon substrate (scan area is $3.0 \times 3.0 \mu\text{m}^2$); **a** and **b** are the height images of PEI-(Ni(NO₃)₂/1)₅ ($R_{\text{rms}} = 2.11 \text{ nm}$) and PEI-(Ni(NO₃)₂/1)₁₀ ($R_{\text{rms}} = 6.17 \text{ nm}$), respectively

3.4 Scanning Electron Microscope of the Multilayer Films

3.4.1 Scanning Electron Microscope of the (PdCl₂/1)_n Films

The SEM image of (PdCl₂/1)₁₀ film confirmed the rough surface texture. As shown in Fig. 7a, the colloid-like particles are distributed in the film, and the holes with different size and depth are presented on the film surface, which are consistent with the AFM discussed above. Statistic calculations in SEM showed that the particle sizes ranged from 25.0 to 61.1 nm with average size of 37.8 nm (Fig. 7b). EDS spectrum confirmed all the expected elements (Pd, Cl, C and N) on the film (Fig. 7a, inset), which indicated PdCl₂ and complex 1 were adsorbed on the substrates. It should be noted that the presence of Si, O and Pt are most likely from single-crystal silicon substrate and platinum spray used in this procedure. Besides, FT-IR spectrum of (PdCl₂/1)_n film was also investigated. As shown in Fig. S10, a strong broad absorption band centred at $3,400 \text{ cm}^{-1}$ can be assigned to the O–H stretching vibrations of water molecules stemming from air. The shoulder peak at $2,922 \text{ cm}^{-1}$ and sharp band at $1,567 \text{ cm}^{-1}$ are attributed to C–H and C=C (or C=N) stretching vibrations in-plane on the aromatic ring, respectively. The peaks at $1,409 \text{ cm}^{-1}$ and 650 cm^{-1} correspond to C–H bending vibrations on ethyl group and aromatic ring, respectively. The FT-IR spectrum of (PdCl₂/1)_n film indicates the existence of complex 1.

The PdCl₂/1 complexes were prepared by mixing pre-determined quantitative homogeneous solutions of PdCl₂ and complex 1, and characterized by SEM, TEM and EDS to better understand the nature, size and structure of the composite. SEM showed that the particles are relatively uniform in size (Fig. 8a). Statistic calculations in SEM showed the diameters of PdCl₂/1 complex particles ranged from 34.8 to 71.6 nm with average size of 47.5 nm (Fig. 8b). EDS spectrum analysis of the complex reveals the presence of all the expected elements Pd, Cl, C, N (see inset of Fig. 8c), indicating that the complexes in the film

Fig. 7 **a** The SEM image of PEI-(PdCl₂/1)₁₀ film (Inset: EDS spectrum); **b** particle size distribution

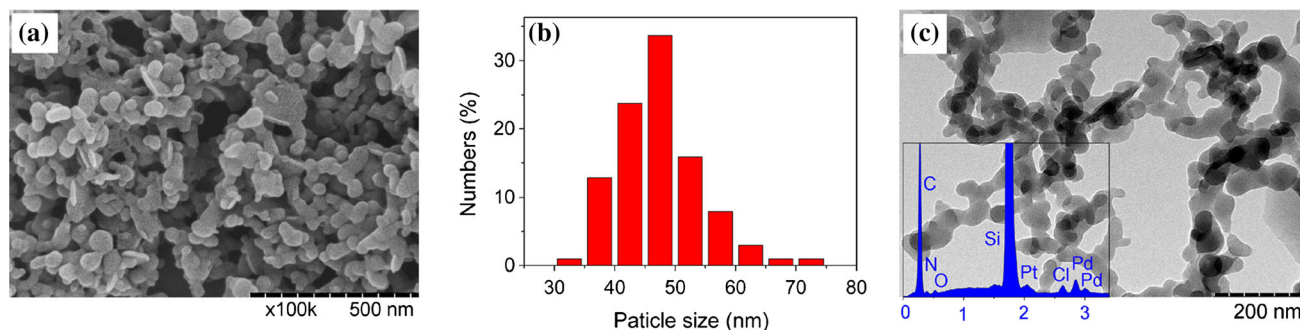
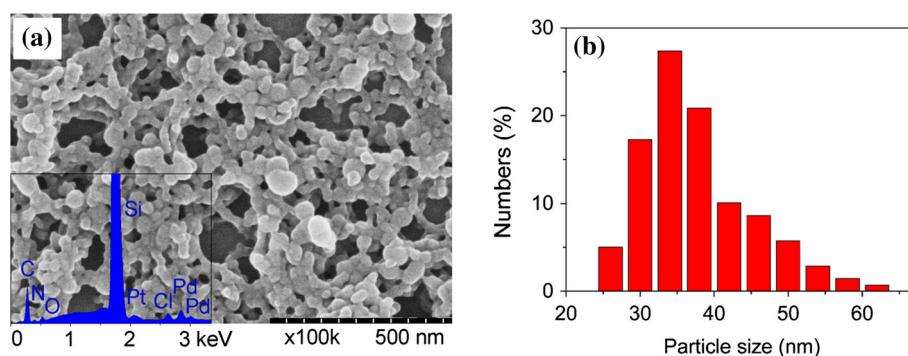


Fig. 8 **a** SEM and **c** TEM images of the PdCl₂/1 complex (Inset: EDS spectrum); **b** particle size distribution

consist of PdCl₂ and complex **1**. The morphologies of PdCl₂/1 complex particles were confirmed by TEM (Fig. 8c).

PdCl₂/1 complex was also characterized by UV–vis absorption spectroscopy, fluorescence spectroscopy, FT-IR spectroscopy and PXRD. The UV–vis absorption spectra (Fig. S11) analysis reveals that compound **1** exhibits absorption peaks at 228 and 330 nm in the solution of EtOH, corresponding to the $\pi \rightarrow \pi^*$ and $n \rightarrow \pi^*$ transitions, respectively; PdCl₂/1 complex shows a broad absorption band centered at 375 nm with a red shift of 25 nm stemming from MLCT transitions, which confirms that PdCl₂/1 complex is composed of PdCl₂ and **1**. The fluorescence emission spectra (Fig. S12) analysis of free **1** and PdCl₂/1 complex also confirms that. IR absorption peaks (Fig. S13) of PdCl₂/1 complex are as follows: 3450 (O–H), 2924 (C–H), 1611 (C=C, C=N), 1218 (C–N), 1154 (C–H), 814 (C–H) cm⁻¹, indicating the presence of complex **1**. Besides, PXRD patterns of PdCl₂/1 complex are likely a mix of PdCl₂ and free **1** (Fig. S14), indicating that the complex is composed of PdCl₂ and **1**.

3.4.2 Scanning Electron Microscope of the (Ni(NO₃)₂/1)_n Films

The SEM images of (Ni(NO₃)₂/1)₁₀ film were recorded to understand the surface morphology. As shown in Fig. 9a,

the islanded-like particles were distributed in the film with different size and depth, indicating the rough surface texture, which were consistent with the AFM discussed above. EDS spectrum confirmed all the expected elements (Ni, C, N and O) on the film (Fig. 9a, inset), which proved Ni(NO₃)₂ and complex **1** were adsorbed on the substrates. The peaks of Si, Al and Pt are derived from the single-crystal silicon substrate and platinum spray used in this procedure, respectively. Statistic calculations indicated that the particle size in the films ranged from 35.9 to 63.7 nm with mean size of 49.7 nm (Fig. 9b). Besides, IR absorption peaks (Fig. S15) of (Ni(NO₃)₂/1)_n film are as follows: 3446 (O–H), 2920 (C–H), 1652 (C=C, C=N), 1385 (C–H), 669 (C–H) cm⁻¹, indicating the presence of complex **1**.

Correspondingly, the (Ni(NO₃)₂/1) complexes were characterized by SEM, TEM and EDS. As shown in Fig. 10, the complexes were rod-like in shape, which were different ones from the film. The element map gave all the expected elements Ni, C, N and O measured by EDS spectrum (Fig. 10b, inset), indicating that the (Ni(NO₃)₂/1) complex should be composed of Ni(NO₃)₂ and complex **1**.

Besides, the UV–vis absorption spectroscopy, fluorescence spectroscopy, FT-IR spectroscopy and PXRD could also give some evidences concerning the nature of (Ni(NO₃)₂/1) complex. The UV–vis absorption spectra (Fig. S11) analysis reveals that (Ni(NO₃)₂/1) complexes show two absorption peaks at 212 and 332 nm, which are

Fig. 9 **a** The SEM image of PEI-(Ni(NO₃)₂/1)₁₀ film (*Inset*: EDS spectrum); **b** particle size distribution

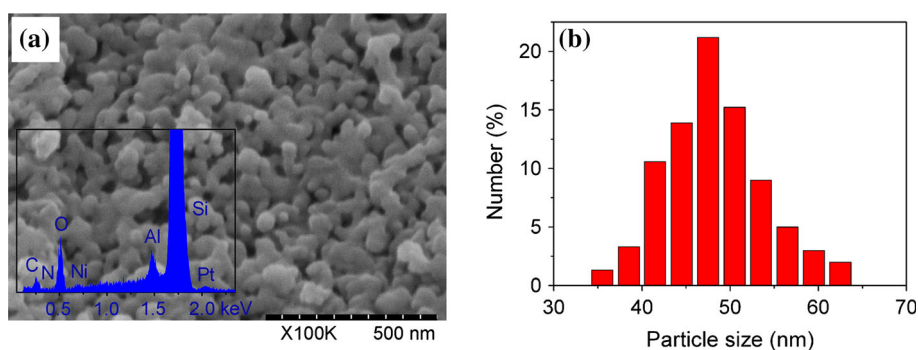
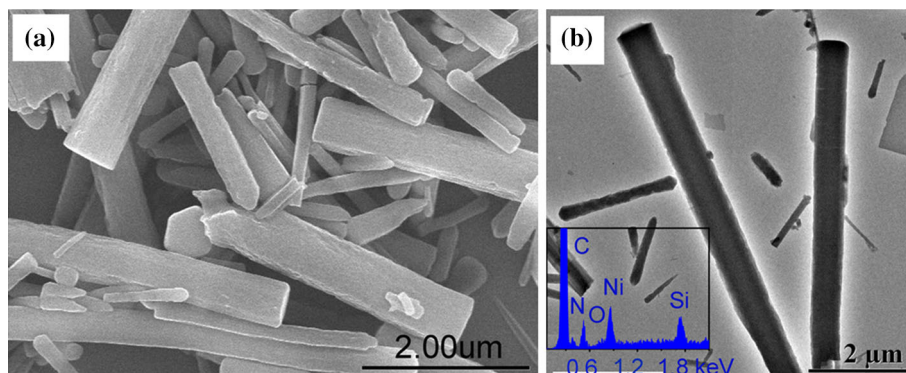


Fig. 10 **a** SEM and **b** TEM images of Ni(NO₃)₂/1 complex (*Inset*: EDS spectrum)



similar with the corresponding peaks of complex **1**. The shift of the highest absorption peak between Ni(NO₃)₂/1 complexes and free **1** may be attributed to MLCT transitions. This inference is also tested and proved by fluorescence emission spectra of the relevant samples in the same solution of EtOH (Fig. S12). Besides, IR absorption peaks (Fig. S16) of Ni(NO₃)₂/1 complex are as follows: 3419 (O–H), 2963 (C–H), 1612 (C=C, C=N), 1384 (C–H), 814 (C–H) cm⁻¹, indicating the presence of complex **1**. PXRD patterns of Ni(NO₃)₂, complex **1** and Ni(NO₃)₂/1 complex were also recorded (Fig. S17), which clearly showed that the pattern of Ni(NO₃)₂/1 complex was the stack of Ni(NO₃)₂ and free **1**.

3.5 Catalytic Application of the (PdCl₂/1)₁₀ Films Loaded Quartz Slide for the Suzuki–Miyaura Cross-Coupling Reaction

In order to optimize the efficiency of (PdCl₂/1)₁₀ multilayer film as catalysts, the Suzuki–Miyaura reaction of 4-bromoanisole with phenylboronic acid was carried out under a variety of time conditions, and the results are presented in Table S1. Among the time employed, 1 h gives the very low yield (18 %). 2 h offers moderate yield (56 %). When the time increased to 4 h, the high yield (96 %) was obtained.

To explore the scope of the catalytic reactions, the cross-couplings between aryl halides and arylboronic acid were

carried out with K₂CO₃ as base in H₂O/EtOH at 50 °C for 4 h. As shown in Table 1, the *para*-substituted aryl bromides with electron-withdrawing (e.g., 4-CF₃, 4-CN, 4-COMe) and electron-donating groups (e.g., 4-OMe) give the corresponding biaryls in high yields. However, the *ortho* substituents offer the low yield due to the steric hindrance effect (Table 1, entry 7). Longer reaction time and higher temperature were required for complete conversion (Table 1, entry 8). The *para*-substituted arylboronic acids bearing electron-donating substituents (e.g., 4-Me, 4-OMe) also favor the coupling reactions (Table 1, entries 9–10). Even for the *ortho*-substituted arylboronic acid (e.g., 2-MeO), it also gives high yield (Table 1, entry 11), indicating that the steric hindrance effect from the *ortho* substituents hardly affects the yield of the reactions.

In order to further investigate the catalytic activity of the (PdCl₂/1)₁₀ films, a series of parallel experiments were performed in the similar conditions. It was observed that complex **1** as a catalyst was inactive in the reaction of 4-methoxy-aryl bromide and phenylboronic acid without the palladium source (Table S2, entry 1). Contrarily, PdCl₂ displayed moderate catalytic activity with the yield of 55 % (Table S2, entry 2). Reaction of PdCl₂ with **1** formed a precipitate, which was collected and fully characterized. The PdCl₂/1 complex exhibited relatively higher catalytic activity than PdCl₂, but less than the (PdCl₂/1)₁₀ films (Table S2, entries 3 and 4). Besides, this film as catalyst can be successfully re-used for several times, and high

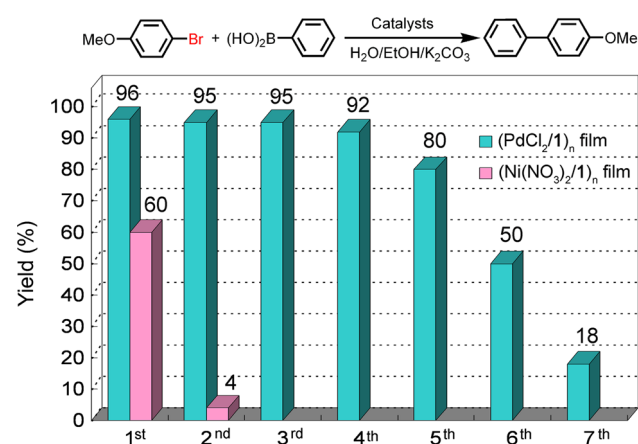
Table 1 Suzuki-Miyaura cross-coupling reactions of aryl halides with arylboronic acid using $(\text{PdCl}_2/\mathbf{1})_{10}$ films loaded on quartz slides as catalysts

Entry	R ₁	R ₂	X	T/ °C, timer/h	Yield (%) ^a
1	4-OEt	Me	I	50, 4	97
2	H	H	Br	50, 4	89
3	4-CF ₃	H	Br	50, 4	87
4	4-CN	H	Br	50, 4	95
5	4-COMe	H	Br	50, 4	93
6	4-OMe	H	Br	50, 4	96
7	2-OMe	H	Br	50, 4	55
8	2-OMe	H	Br	100, 24	86
9	H	4-Me	Br	50, 4	95
10	H	4-OMe	Br	50, 4	95
11	H	2-OMe	Br	50, 4	90

General procedure: 1.0 mmol of aryl halide, 1.2 mmol of arylboronic acid, 3 mmol of K₂CO₃, in H₂O/EtOH (4:3, V/V) under ambient atmosphere

^a Isolated yield. ¹H NMR data of the products in Supplementary Materials

yields of the coupled products were obtained under similar conditions (Fig. 11, or Table S3, entries 1–5). After five cycles, the yield decreased rapidly (Table S3, entries 6–7), indicating that the catalytic active species into the solution were gradually used up in the reactions [15, 17]. Contrastively, $(\text{PdCl}_2/\mathbf{1})_{10}$ films as catalyst for the reaction of 4-iodophenetole with 4-methylphenylboronic acid can be recycled six times (Fig. 12, or Table S4, entries 1–6). Afterword, it sharply lost catalytic activity. After each cycle step, a certain amount of metal–ligand complexes were desorbed from films into reaction mixture, so it is very important to recycle the solvent for the yield and environmental protection.

**Fig. 11** Yields obtained in recycled catalysis runs of reaction of 4-bromoanisole with phenylboronic acid using $(\text{PdCl}_2/\mathbf{1})_n$ and $(\text{Ni}(\text{NO}_3)_2/\mathbf{1})_n$ films as catalysts

3.6 Catalytic Application of the $(\text{Ni}(\text{NO}_3)_2/\mathbf{1})_{10}$ Films Loaded Quartz Slide for the Suzuki–Miyaura Cross-Coupling Reaction

The Suzuki–Miyaura cross-coupling reactions were carried out by employing the $(\text{Ni}(\text{NO}_3)_2/\mathbf{1})_{10}$ multilayer film loaded on the solid slides as catalysts. As shown in Table 2, for aryl iodide, the reaction gives the high yield (entry 1). The aryl bromide offers the low yield of 30 % (Table 2, entry 2), even though longer time and higher temperature are executed in the reaction system, and it is very difficult to reach considerably high yield (Table 2, entry 3), which could be attributed to the low activity of aryl bromide and the low loading of Ni(II) on the film. The Suzuki–Miyaura

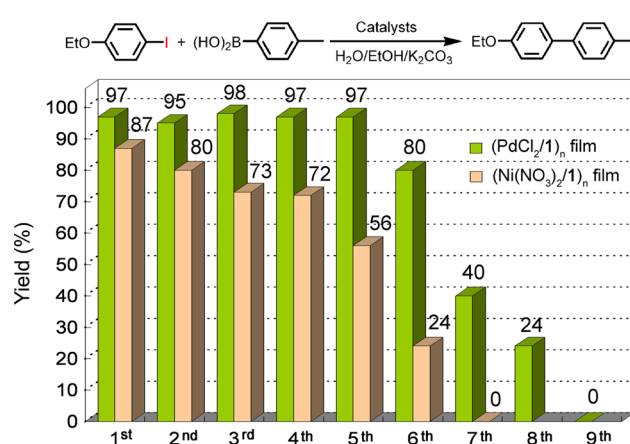
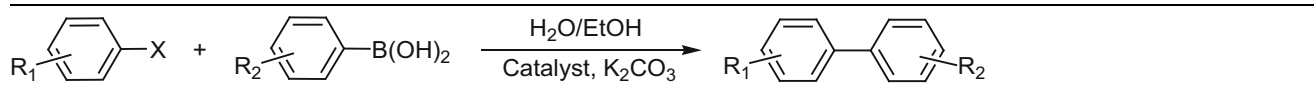
**Fig. 12** Yields obtained in recycled catalysis runs of reaction of 4-iodophenetole with 4-methylphenylboronic acid using $(\text{PdCl}_2/\mathbf{1})_n$ and $(\text{Ni}(\text{NO}_3)_2/\mathbf{1})_n$ films as catalysts

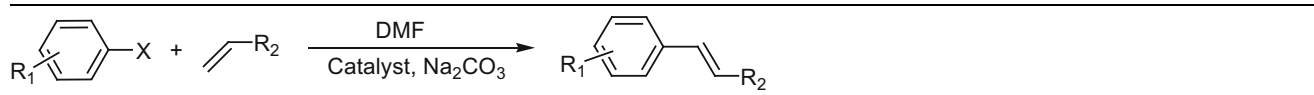
Table 2 Suzuki–Miyaura cross-coupling reactions of aryl halides with arylboronic acid using Ni(NO₃)₂/1 complex and (Ni(NO₃)₂/1)₁₀ films loaded on quartz slides as catalysts


Entry	R ₁	R ₂	X	Catalysts	T/ °C, time/h	Yield (%) ^a
1	4-OEt	4-Me	I	(Ni(NO ₃) ₂ /1) ₁₀ film	90, 10	87 ^b
2	4-OMe	H	Br	(Ni(NO ₃) ₂ /1) ₁₀ film	90, 10	30 ^b
3	4-OMe	H	Br	(Ni(NO ₃) ₂ /1) ₁₀ film	110, 24	60 ^b
4	4-OEt	4-Me	I	Ni(NO ₃) ₂ /1 complex	90, 10	85 ^c
5	4-OMe	H	Br	Ni(NO ₃) ₂ /1 complex	90, 10	81 ^c
6	4-CF ₃	H	Br	Ni(NO ₃) ₂ /1 complex	90, 10	80 ^c

General procedure: 1.0 mmol of aryl halide, 1.2 mmol of arylboronic acid, 3 mmol of K₂CO₃, in H₂O/EtOH (3:4, V/V) under ambient atmosphere

^a Isolated yield

^{b,c} Catalyst loading was 8.5×10^{-5} and 0.03 mmol, respectively. ¹H NMR data of the products in Supplementary Materials

Table 3 Mizoroki–Heck cross-coupling reactions of aryl halides with olefins using (PdCl₂/1)₁₀ and (Ni(NO₃)₂/1)₁₀ films loaded on quartz slides as catalysts


Entry	R ₁	R ₂	X	Catalyst	Yield (%) ^a
1	H	Ph	Br	(PdCl ₂ /1) ₁₀ films	67
2	4-CN	Ph	Br	(PdCl ₂ /1) ₁₀ films	94
3	4-COMe	Ph	Br	(PdCl ₂ /1) ₁₀ films	70
4	4-CF ₃	Ph	Br	(PdCl ₂ /1) ₁₀ films	73
5	4-OMe	Ph	Br	(PdCl ₂ /1) ₁₀ films	78
6	H	COO ^t Bu	Br	(PdCl ₂ /1) ₁₀ films	49
7	H	COO ^t Bu	I	(PdCl ₂ /1) ₁₀ films	98
8	H	Ph	I	(PdCl ₂ /1) ₁₀ films	96
9	4-CN	Ph	Br	(Ni(NO ₃) ₂ /1) ₁₀ films	42
10	4-COMe	Ph	I	(Ni(NO ₃) ₂ /1) ₁₀ films	68

General procedure: the mixture of aryl halide (1.0 mmol), olefins (1.5 mmol), Na₂CO₃ (2 mmol) and DMF (6 mL) were stirred at 140 °C for 24 h under ambient atmosphere

^a Isolated yield. ¹H NMR data of the products in Supplementary Materials

reaction catalyzed by Ni(NO₃)₂/1 complex performs well. The aryl iodide gives the high yield of 85 % (Table 2, entry 4); the *para*-substituted aryl bromides bearing electron-withdrawing (e.g., CF₃) and electron-donating substituents such as OMe offer the well-pleasing yields (Table 2, entries 5–6).

As we all know, recycling experiment is very important for a successful and potential catalytic system. The recycling behaviour of (Ni(NO₃)₂/1)₁₀ films was investigated. As shown in Fig. 11 or Table S3, entries 11, this film gives extremely low yield (4 %) in the second run, indicating that it could not be effectively multi-used in the reaction of 4-bromoanisole with phenylboronic acid. However,

(Ni(NO₃)₂/1)₁₀ films can be re-used five times for the reaction of 4-iodophenetole with 4-methylphenylboronic acid (Fig. 12 or Table S4, entries 10–14). After five cycles, the yield decreased rapidly (Table S4, entries 15–16), indicating that the Ni(II) species into the solution were gradually used up in the reactions.

3.7 Catalytic Application of the Films Loaded Quartz Slides for the Mizoroki–Heck Reaction

The Mizoroki–Heck reaction was carried out employing the solid slide coated with multilayer films as catalysts. In order to optimize the efficiency of films, the effect of time

for the reaction between 4-bromobenzonitrile and styrene is investigated using $(\text{PdCl}_2/\mathbf{1})_{10}$ films as catalyst. As shown in Table S5, the reaction gives the highest yield under 24 h among all the time used.

To further explore the scope of the catalytic reactions, the Mizoroki–Heck cross-coupling reaction between aryl halides and terminal olefins with $(\text{PdCl}_2/\mathbf{1})_{10}$ and $(\text{Ni}(\text{NO}_3)_2/\mathbf{1})_{10}$ films as catalysts were performed. For $(\text{PdCl}_2/\mathbf{1})_{10}$ films, it is evident in Table 3 that aryl bromides containing electron-withdrawing/donating groups (e.g., CN, COMe, CF₃, OMe) give moderate yields (Table 3, entries 2–5). However, in the reaction of bromobenzene and terminal olefins (e.g., COO^tBu), the reaction offers low yield (Table 3, entry 6). The reactions between aryl iodides and olefins (e.g., Ph, COO^tBu) present high yield under the same conditions (Table 3, entries 7). In 2002, Kawano et al. reported that dichloro-(2,2'-bipyridine) palladium(II) complex is not suitable for the Mizoroki–Heck reaction of aryl bromides [34]. However, in our work, the $(\text{PdCl}_2/\mathbf{1})_n$ catalyst with very low loading (ppm level) is proved to be high active for the Mizoroki–Heck reaction of aryl bromides and terminal olefins. Correspondingly, the $(\text{Ni}(\text{NO}_3)_2/\mathbf{1})_{10}$ films-catalyzed Mizoroki–Heck reaction were also performed in this report. The coupling of aryl iodides with styrene gave desired product in moderate yield (Table 3, entry 10), while aryl bromides showed low yield (Table 3, entry 9), because aryl bromides is less active than aryl iodides.

4 Conclusions

Compound **1** was successfully prepared and used in the LbL self-assembly of multilayer films through a sequential reaction with metal ions Pd(II) or Ni(II). The resulting $(\text{PdCl}_2/\mathbf{1})_n$ multilayers were used as high active catalysts for the Suzuki–Miyaura and Mizoroki–Heck reactions with extremely low Pd(II)-loading in ppm level. Interestingly, the $(\text{Ni}(\text{NO}_3)_2/\mathbf{1})_n$ multilayers as the active catalytic moieties can be re-used five times in Suzuki–Miyaura reaction of 4-iodophenetole with 4-methylphenylboronic acid, which is attractive for industrial syntheses in the view of the low costs.

Acknowledgments Authors acknowledge the financial support by the NSFC (21571110), the Ningbo Foundation (2014C50037 and 2014A610106), the Ningbo University Foundation (py2013001, and G14034), the Youth Talent programs of Zhejiang Province

(2013R405068) and sponsored K. C. Wong Magna Fund in Ningbo University.

References

- Suzuki A (1985) *Pure Appl Chem* 57:1749
- Heck RF (1982) *Org React* 27:345
- Milstein D, Stille JK (1979) *J Am Chem Soc* 101:4981
- Milstein D, Stille JK (1979) *J Am Chem Soc* 101:4992
- Milstein D, Stille JK (1979) *J Org Chem* 44:1613
- Yang LM, Huang LF, Luh TY (2004) *Org Lett* 6:1461
- Negishi E (1982) *Acc Chem Res* 15:340
- Erdik E (1992) *Tetrahedron* 48:9577
- Nakao Y, Hiyama T (2011) *Chem Soc Rev* 40:4893
- Sonogashira K, Tohda Y, Hagihara N (1975) *Tetrahedron Lett* 16:4467
- Lipshutz BH, Taft BR (2008) *Org Lett* 10:1329
- Moore LR, Shaughnessy KH (2004) *Org Lett* 6:225
- Liu S, Berry N, Thomson N, Pettman A, Hyder Z, Mo J, Xiao L (2006) *J Org Chem* 71:7467
- Battace A, Zair T, Doucet H, Santelli M (2006) *Synthesis* 3495
- Gao SY, Huang YB, Cao MN, Liu TF, Cao R (2011) *J Mater Chem* 21:16467
- Tucker CE, de Vries JG (2002) *Top Catal* 19:111
- Gao SY, Zheng ZL, Lu J, Cao R (2010) *Chem Commun* 46:7584
- Sigeev AS, Peregodov AS, Cheprakov AV, Beletskaya IP (2015) *Adv Synth Catal* 357:417
- Basu B, Paul S (2013) *Appl Organometal Chem* 27:588
- Ye M, Gao GL, Yu JQ (2011) *J Am Chem Soc* 133:6964
- Özdemir İ, Cetinkaya B, Demir S, Gürbüz N (2004) *Catal Lett* 97:37
- Li X, Zhao XH, Gao SY, Marqués-González S, Yufit DS, Howard JAK, Low PJ, Zhao YY, Gan N, Guo ZY (2013) *J Mater Chem A* 1:9164
- Li X, Zhao XH, Zhang J, Zhao YY (2013) *Chem Commun* 49:10004
- Wang M, Yuan XB, Li HY, Ren LM, Sun ZZ, Hou YJ, Chu WY (2015) *Catal Commun* 58:154
- Zim D, Monteiro AL (2002) *Tetrahedron Lett* 43:4009
- Altman M, Shukla AD, Zubkov T, Evmenenko G, Dutta P, van der Boom ME (2006) *J Am Chem Soc* 128:7374
- Altman M, Zenkina OV, Ichiki T, Iron MA, Evmenenko G, Dutta P, van der Boom ME (2009) *Chem Mater* 21:4676
- Motiei L, Altman M, Gupta T, Lupo F, Gulino A, Evmenenko G, Dutta P, van der Boom ME (2008) *J Am Chem Soc* 130:8913
- Altman M, Zenkina O, Evmenenko G, Dutta P, van der Boom ME (2008) *J Am Chem Soc* 130:5040
- Choudhury J, Kaminker R, Motiei L, de Ruiter G, Morozov M, Lupo F, Guilino A, van der Boom ME (2010) *J Am Chem Soc* 132:9295
- Milie TN, Chi N, Yablon DG, Flynn GW, Batteas JD, Drain CM (2002) *Angew Chem Int Ed* 41:2117
- Milic T, Gamo JC, Batteas JD, Smeureanu G, Drain CM (2004) *Langmuir* 20:3974
- Li X, Zha MQ, Wang XW, Cao R (2009) *Inorg Chim Acta* 362:3357
- Kawano T, Shinomaru T, Ueda I (2002) *Org Lett* 4:2545